DIGITAL ACCESS TO SCHOLARSHIP AT HARVARD
DASH.HARVARD.EDU

HARVARD LIBRARY
Office for Scholarly Communication

Solute Trapping of Ge in Al

Citation
Smith, Patrick M., Jeffrey A. West, Michael J. Aziz. 1992. Solute Trapping of Ge in Al. Materials Research Society Symposia Proceedings 205: 331-336.

Published Version
http://www.mrs.org/s_mrs/sec.asp?CID=1727&DID=38980

Permanent link
http://nrs.harvard.edu/urn-3:HUL.InstRepos:2870695

Terms of Use
This article was downloaded from Harvard University's DASH repository, and is made available under the terms and conditions applicable to Other Posted Material, as set forth at http://nrs.harvard.edu/urn-3:HUL.InstRepos:dash.current.terms-of-use#LAA

Share Your Story

The Harvard community has made this article openly available.
Please share how this access benefits you. Submit a story .

Accessibility

SOLUTE TRAPPING OF GE IN AL

PATRICK M. SMITH, JEFFREY A. WEST, AND MICHAEL J. AZIZ
Division of Applied Sciences, Harvard University, Cambridge MA 02138

ABSTRACT

Partitioning during rapid solidification of dilute Al-Ge alloys has been investigated. Implanted thin films of Al have been pulsed-laser melted to obtain solidification at velocities in the range of 0.01 m/s to 3.3 m/s, as measured by the transient conductance technique. Previous and subsequent Rutherford Backscattering depth profiling of the Ge solute in the Al alloys has been used to determine the nonequilibrium partition coefficient k. A significant degree of lateral film growth during solidification confines determination of k to the placing of an upper bound of 0.22 on k for solidification velocities in this range. We place a lower limit of 10 m/s on the "diffusive velocity," which locates the transition from solute paritioning to solute trapping in the Continuous Growth Model.

INTRODUCTION

Trapping of various solutes in silicon during rapid solidification has been observed in the past, and models have been developed [1,2] which satisfactorily explain the transition from solute partitioning at low solidification velocities to solute trapping at higher solidification velocities. However, measurements of solute trapping during rapid solidification have not been made for metallic systems, and it is not known whether or not the models developed for trapping in semiconductors can be applied to metallic systems. Furthermore, it is not even known at what velocities the transition might occur in metallic systems.

The degree of solute trapping is defined by the partition coefficient k, which is the ratio of the concentration of solute in the solid c_s to the solute concentration in the liquid c_l immediately in front of the advancing solid/liquid interface:

$$k = \frac{c_s}{c_l} \tag{1}$$

One model which has been frequently used in rapid solidification calculations is the Continuous Growth Model (CGM) of Aziz and Kaplan [1], which predicts the following dependence of the partition coefficient k on the solidification velocity v for low solute concentrations:

$$k(v) = \frac{v/v_d + k_e}{v/v_d + 1} \tag{2}$$

The transition from equilibrium partitioning ($k = k_e$) to complete trapping ($k = 1$) is centered at the "diffusive velocity" v_d, as shown in Figure 1.

At present there is no reliable method of determining v_d by any means other than fitting to a measured $k(v)$ relation. A common assumption is that the diffusive velocity can be approximated by the diffusivity D_L of the solute in the bulk liquid solvent divided by an "interface width" L, which corresponds to the region in which interactions between atoms are dictated by the nature of the liquid/solid interface, and not by bulk material properties. If this were true, one would expect that for small solute concentrations, the "interface width" L should not depend on the nature of the solute. However, experiments examining trapping of Bi [3], Sn [4], and Ge [5] in Si indicate that the "interface width" determined in this manner is far from constant.

MJA '84

Values for the "interface width" calculated from experimentally obtained diffusive velocities and liquid diffusivities are listed in Table I; these values vary by almost two orders of magnitude. Obviously, v_d is dependent on more than the width of the liquid/solid interface for Si. It is therefore important to determine v_d for several systems in order to gain more insight into its nature.

We have chosen to investigate solute trapping in the Al-Ge system for several reasons: 1) The equilibrium value k_e of the partition coefficient is only 0.05, so the transition to $k = 1$ (solute trapping) should be easily identified. 2) The Al-Ge phase diagram is a simple binary eutectic, with no stoichiometric compounds present. 3) Aluminum films behave very well in transient conductance experiments, which allows measurement of the solidification velocity [6].

Table I: *Experimentally determined "interface widths" L for various solutes in Si.*

	Bi in Si	Sn in Si	Ge in Si
measured D_L	2×10^{-4} cm^2/s	2.5×10^{-4} cm^2/s	4×10^{-4} cm^2/s
measured v_d	32 m/s	17 m/s	1 m/s
inferred $L = D_L/v_d$	6 Å	15 Å	400 Å

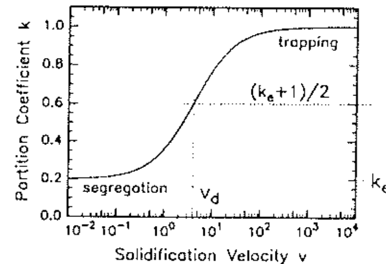

Figure 1: *Dependence of partition coefficient on solidification velocity in the Continuous Growth model, in a system with an equilibrium partition coefficient of $k_e = 0.2$. The transition from solute partitioning to solute trapping is centered at the diffusive velocity v_d.*

THE EXPERIMENT

The Transient Conductance Measurement (TCM) technique [7,8], developed to study rapid solidification in silicon, has been successfully applied to solidification studies in pure aluminum [6]. This technique affords the advantage of one-dimensional melting and regrowth, which makes analysis of the solidified solute profiles tractable. The absence of lateral thermal gradients and the thinness of the Al film prevent convection while the film is molten. Applying the TCM technique to metallic systems is more difficult because the changes in the electrical and optical properties accompanying melting and solidification are much smaller for metals than for semiconductors. When silicon is melted, it becomes metallic, with a resulting drop in its resistivity by a factor of 30 [8]; metals, however, exhibit changes in resistivity of only a factor of 1 to 3 upon melting (the resistivity of Al increases by a factor of 2.2 when melted [6]). The reflectivity of silicon increases upon melting, thus mitigating the effects of any lateral non-uniformities in the laser beam. Unfortunately, the reflectivity of most metals decreases upon melting; the effects of any hot spots in the laser beam are therefore amplified. Transient conductance experiments with metals therefore require a more spatially uniform laser pulse than do the same experiments with semiconductors. However, since absorption in metals is higher for ultraviolet light than for visible light, the ratio of the liquid to solid absorptions is closer to unity for XeCl (308 nm) excimer laser irradiation. Thus the effects of non-uniformities in the excimer laser pulse are not as important as those produced by inhomogenieties in visible light laser pulses.

We deposited 2800 Å aluminum films by electron-beam evaporation on 1.1 μm thermally oxidized silicon wafers. A thin (~70 Å) layer of Cr was deposited before the aluminum film to promote adhesion and to act as a seed for regrowth should the aluminum film be completely melted during the experiment. These films were then ion implanted with $^{76}Ge^+$ at 60 keV to a dose of 6×10^{15} atoms/cm^2, which results in an implant profile with a peak concentration of about 1.0 atomic percent at a depth of 400 Å (the average Ge concentration in the 2800 Å Al film is about 0.4%). After implantation the Al films were photolithographically patterned to form serpentine thin film wire resistors 5.3 mm long, with a length to width ratio of 75 ± 6. These Ge-implanted Al films had room temperature resistances of $10.5 \pm 0.6\,\Omega$, corresponding to average resistivities of 3.9 $\mu\Omega$-cm.

The samples were then melted with a 30 ns FWHM XeCl (308 nm) excimer laser pulse in the transient conductance experiment configuration shown schematically in Figure 2. The laser pulse energy incident on the sample was varied between 0.31 and 0.75 J/cm^2. A typical transient conductance trace is shown in Figure 3, along with the method for calculating the solidification velocity; these were calculated by determining the times at which solidification began and finished. Calculation of the solidification velocity was then straightforward, as the film thicknesses were measured by Rutherford Backscattering Spectrometry (RBS). Heat flow simulations for these samples indicate that the solidification velocity does not vary by more than about 20% during solidification.

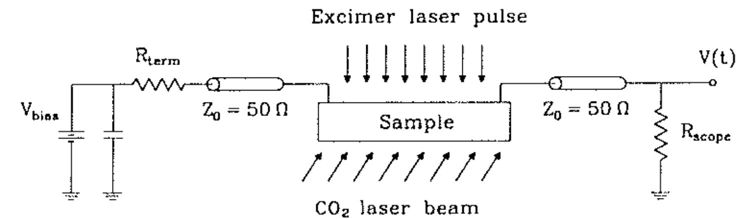

Figure 2: *Transient Conductance experiment [8]. The sample is heated from behind by a CO_2 laser prior to melting with the excimer laser pulse. Resistors R_{term} and R_{scope} are matched to the cable impedance Z_0 to supress signal reflections. With a DC voltage V_{bias} applied to sample, one can use the measured voltage V(t) to calculate the sample resistance as a function of time.*

To obtain slower solidification velocities, the samples were heated from behind with a 80 watt CO_2 laser prior to the firing of the excimer laser; this allowed us to raise the sample temperature as high as the melting point of aluminum (660°C) within 1.4 seconds or less. By heating the samples, we were able to lower the solidification velocity from 3.3 m/s to 0.01 m/s. Melt durations ranged from 440 ns (for the fastest solidification) to 35 μs (for the slowest solidification).

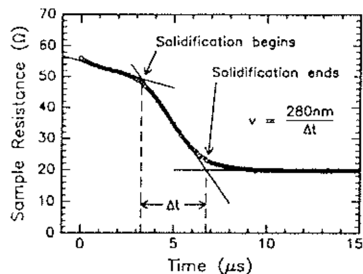

Figure 3: *Example transient conductance trace for a 2800Å Al sample. Excimer laser fires at t=0 μs, melting entire Al film; liquid cools until about 3.2 μs, when solidification begins. Solidification continues for Δt, after which the hot solidified film cools.*

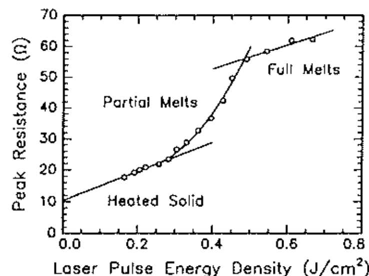

Figure 4: *Plot of maximum resistance reached by several samples irradiated at varying laser powers shows three distinct regions: heating of the solid Al film, incomplete melting of the film, and complete melting.*

RESULTS

Solute depth profiles were obtained by RBS in a grazing-exit geometry (110° scattering angle); various ^{76}Ge depth profiles are shown in Figure 5. For velocities below about 1.0 m/s, large surface excesses of ^{76}Ge are observed, indicating solute partitioning during solidification toward the surface of the sample. At higher solidification velocities, the surface peaks become smaller, and eventually disappear.

The area of the surface peak after solidification is equal to the area of the "diffusive spike" of solute being pushed ahead of the interface during solidification, which, under steady-state conditions, is the product of the spike's height and width. The height of the spike is $c_l - c_s$, which is proportional to $((1/k) - 1)$; hence as k increases toward unity the area vanishes. Additionally, the width of the spike varies inversely with velocity (unlike the width of the experimentally measured surface peak, which is determined by the energy resolution of the RBS detector). Under steady-state solidification conditions, the relative contributions of these two effects to the observed velocity dependence of the size of the surface peak can be determined analytically. Rather than risk potential errors due to the steady state approximation, we used a full one-dimensional numerical simulation of diffusion and partitioning during solidification [3,9,10] and compared the result to measured depth profiles. These simulations, given a measured initial solute profile, a measured time-dependence of the melt depth, and values for the bulk liquid diffusivity D_L and the partition coefficient k, solve the diffusion equation to obtain the final solute depth profile after melting and resolidification. Comparison of the simulation to measured final depth profiles allows a unique determination of both D_L and k. The liquid diffusivity D_L of Ge in liquid Al was determined by simulating the diffusion of solute in the liquid for times corresponding to the shortest melt durations seen in the experiment; samples with longer melt durations showed a completely homogeneous Ge distribution in the Al film.

As shown in Figure 6, the apparent partition coefficient does not vary by more than ± 0.10 over the range of solidification velocities investigated, with an average value of $k = 0.22$. This is significantly larger than the equilibrium value of $k_e = 0.05$. Preliminary plan-view transmission electron microscopy of one of the more rapidly solidified samples showed Al grains ranging in size from 1 μm to 5 μm. There is no evidence of cellular growth, which we have seen for larger Ge concentrations (15 atomic percent) in 1300Å Al films. Since the observed grain size is much larger than the film thickness (about 0.3 μm), we assume that significant lateral growth has taken

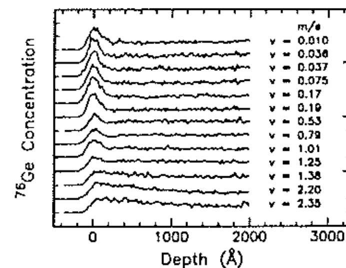

Figure 5: *^{76}Ge depth profiles determined by Rutherford Backscattering for various solidification velocities. Profiles are offset vertically.*

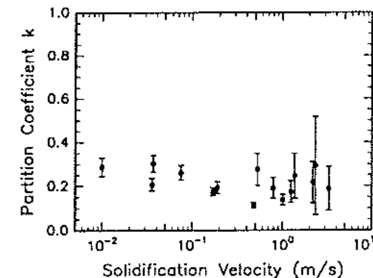

Figure 6: *Values of the partition coefficient for dilute solutions of Ge in Al for a range of solidification velocities, determined by fitting profiles in figure 5 with one-dimensional diffusion and solidification simulations.*

place during solidification. Evidently the thin Cr backing layer between the deposited aluminum film and the SiO_2 did not provide enough nucleation sites for the aluminum layer to nucleate and regrow in a planar fashion. Such lateral growth would segregate Ge laterally, with the result that some of the segregated Ge would appear deep in the film along grain boundaries. Since smaller values of the partition coefficient yield larger surface excesses of solute (at constant solidification velocity), we interpret the partition coefficients deduced in figure 6 to be *upper bounds* on k. Since k is still small (much less than unity) at the fastest solidification observed (3 m/s), the transition to trapping (at $k = 1$) has not begun, and we can place a lower limit of 10 m/s on the diffusive velocity v_d in equation (2).

To circumvent the problems of non-planar solidification, we plan to melt deep into the Al films, without melting the entire film; this will allow enough time for solute diffusion in the liquid without requiring that Al nucleate from the substrate. In addition, in order to probe solute trapping behavior at higher solidification velocities, substrates with thinner insulating oxide layers will be used to provide faster heat conduction away from the Al film. Other substrate materials with higher thermal conductivities may also be used to allow faster regrowth velocities.

SUMMARY

We have used the Transient Conductance Measurement technique to measure solidification velocities in metals, and have used subsequent RBS depth profiling and solidification simulations to extract $k(v)$. Apparent values of k remain at 0.22 ± 0.10 over the range of solidification velocities from 0.01 m/s to 3.3 m/s; this is significantly above the equilibrium value k_e of the partition coefficient, but well below unity. This result and preliminary TEM are interpreted as indications of non-planar growth, which would imply that the values obtained for k are upper limits. As the partition coefficient remains low at velocities as high as 3 m/s, we place a lower limit of 10 m/s on the diffusive velocity v_d in dilute Al-Ge alloys.

ACKNOWLEDGEMENTS

The authors thank John Elmer and Jeff Kass of Lawrence Livermore National Laboratory for providing facilities for ion implantation, and Yuan Lu of Harvard University for assistance with electron microscopy. This research was supported by the U.S. D.O.E. under grant DE-FG02-89ER45401 (J. B. Darby).

REFERENCES

[1] Michael J. Aziz and Thoedore Kaplan, *Acta. metall.* **36**, 2335 (1988).
[2] L. M. Goldman and M. J. Aziz, *J. Mater. Res.* **2** 524 (1987).
[3] M. J. Aziz, J. Y. Tsao, M. O. Thompson, P. S. Peercy, and C. W. White, *Phys. Rev. Lett.* **56**, 2489 (1986).
[4] D. E. Hoglund, M. J. Aziz, S. R. Stiffler, M. O. Thompson, J. Y. Tsao, and P. S. Peercy, *Acta. metall.*, in press.
[5] M. J. Aziz, J. Y. Tsao, M. O. Thompson, P. S. Peercy, C. W. White, and W. H. Christie, *Mater. Res. Soc. Proc.* **35**, 153 (1985).
[6] J. Y. Tsao, S. T. Picraux, P. S. Peercy, Michael O. Thompson, *Appl. Phys. Lett.* **48**, 278 (1986).
[7] G. J. Galvin, Michael O. Thompson, J. W. Mayer, R. B. Hammond, N. Paulter, and P. S. Peercy, *Phys. Rev. Lett.* **48**, 33 (1982).
[8] Michael O. Thompson, *PhD. Thesis*, Cornell University, 1984.
[9] Computer simulations were adapted from code provided by M. O. Thompson of Cornell University.
[10] P. Baeri and S. U. Campisano, in *Laser Annealing of Semiconductors*, edited by J. M. Poate and James W. Mayer (Academic Press, New York, 1982), chapter 4.

CRYSTAL FACE DEPENDENT MELTING OF A POLYCRYSTALLINE IRON SURFACE DURING 30 PS LASER PULSES

A. Vaterlaus, D. Guarisco, and F. Meier
Laboratorium für Festkörperphysik, ETH Hönggerberg, 8093 Zürich, Switzerland

ABSTRACT

The melting of a polycrystalline iron surface with short laser pulses induces a surface structure with an orientation and a morphology depending on the crystal face of the surface. Different crystal planes irradiated with the same laser pulses show different degrees of disorder. This points to a crystal face dependent surface melting temperature.

INTRODUCTION

High intensity laser pulses hitting a sample surface can induce periodic surface structures. The rippling of the surface occurs with a corrugation and a morphology which depends on the degree of surface melting of the sample [1,2]. For normal incidence the orientation of the ripples is generally found to be perpendicular to the E - vector of the linear polarized light [3,4]. However scratches and other surface irregularities being present in the laser focus also influence or determine the orientation of the structures [5,6]. Only for a Ge(111) surface the symmetry of the LIPSS (laser induced periodic surface structure) was found to be related to the symmetry of the crystal surface [3].

The investigation of the LIPSS induced on a polycrystalline sample with crystallites of appropriate size offers the possibility to investigate the LIPSS orientation for different crystal faces irradiated with the same laser pulses. Furthermore different surface melting temperatures of the crystallites should result in different morphologies of the induced ripples.

EXPERIMENT

A polycrystalline Fe sample (cylinder with: l = 5mm and d = 5 mm) was polished with diamond paste down to a roughness of 0.1 µm. After insertion into the UHV system which is normally used for a photoemission experiment [7], the surface of the sample was cleaned by cycles of Ar ion sputtering and heating. This treatment produced a clean surface with a few percent of carbon being the only contamination detected by the Auger spectroscopy. The LIPSS have been induced with 30 picosecond laser pulses at normal incidence. A photon energy of 2.15 eV (570 nm) was used. The degree of linear polarization was 67 %. With the same laser pulses used for the LIPSS formation a spin polarized photoemission experiment was performed to investigate the time scale of the spin - lattice relaxation process. In order to make the emission of the photoelectrons possible the work function of the iron was lowered by deposition of about 0.5 ML of Cs